European Journal of Immunology

Adaptive immunity

Basic

Research Article

Human T cells employ conserved AU-rich elements to fine-tune IFN-γ production

Julian J. Freen-van Heeren[1,2], *Branka Popović*[1,2], *Aurélie Guislain*[1,2] *and Monika C. Wolkers*[1,2]

[1] Department of Hematopoiesis, Sanquin Research-Amsterdam UMC Landsteiner Laboratory, Amsterdam, The Netherlands
[2] Department of Hematopoiesis, Oncode Institute, Amsterdam, The Netherlands

Long-lasting CD8$^+$ T cell responses are critical in combatting infections and tumors. The pro-inflammatory cytokine IFN-γ is a key effector molecule herein. We recently showed that in murine T cells the production of IFN-γ is tightly regulated through adenylate uridylate–rich elements (AREs) that are located in the 3′ untranslated region (UTR) of the *Ifng* mRNA molecule. Loss of AREs resulted in prolonged cytokine production in activated T cells and boosted anti-tumoral T cell responses. Here, we investigated whether these findings can be translated to primary human T cells. Utilizing CRISPR-Cas9 technology, we deleted the ARE region from the *IFNG* 3′ UTR in peripheral blood-derived human T cells. Loss of AREs stabilized the *IFNG* mRNA in T cells and supported a higher proportion of IFN-γ protein-producing T cells. Importantly, combining MART-1 T cell receptor engineering with ARE-Del gene editing showed that this was also true for antigen-specific activation of T cells. MART-1-specific ARE-Del T cells showed higher percentages of IFN-γ producing T cells in response to MART-1 expressing tumor cells. Combined, our study reveals that ARE-mediated posttranscriptional regulation is conserved between murine and human T cells. Furthermore, generating antigen-specific ARE-Del T cells is feasible, a feature that could potentially be used for therapeutical purposes.

Keywords: AU-rich elements · Human · IFN-γ, Posttranscriptional regulation · T cells

Additional supporting information may be found online in the Supporting Information section at the end of the article.

Introduction

CD8$^+$ T cells are critical for immunosurveillance and for the protection against invading pathogens. To do so, they produce effector molecules, including granzymes, chemokines, and cytokines. Interferon γ (IFN-γ) is a key cytokine for CD8$^+$ T cells to exert their effector function [1–3]. IFN-γ is a pleiotropic cytokine that modulates angiogenesis, hematopoiesis, myelopoiesis, and immune cell functions [4–7]. For instance, IFN-γ can suppress the growth of pathogens through upregulation of antiviral factors [8], and attract myeloid cells such as neutrophils to the site of infection [9, 10]. Furthermore, IFN-γ sensing potentiates the innate immune response of dendritic cells, macrophages, monocytes, and neutrophils against (intra)cellular pathogens [9–13]. Indeed, point mutations and deletions in humans in the receptors for IFN-γ, *IFNGR1*, and *IFNGR2*, which often lead to premature stop codons, revealed that IFN-γ sensing is instrumental to protect the host from infections by *Mycobacteria* species [14–16].

IFN-γ also prevents the development of cancers. Mice that lack the *Ifng* gene, or the signaling protein downstream of IFNGR1/2,

Correspondence: Monika C. Wolkers
e-mail: m.wolkers@sanquin.nl

STAT1, spontaneously develop tumors [17, 18]. Furthermore, a high IFN-γ-mediated gene signature correlates with clinical response rates to immunotherapy in humans [19, 20]. Conversely, copy number alterations of IFN-γ pathway genes correlate with a poor response to immunotherapy [21].

The regulation of IFN-γ production is multilayered. The *IFNG* locus is only demethylated in effector and memory T cells [22], allowing for locus accessibility and transcription upon T cell activation. While the production of T cell effector molecules has been mainly attributed to changes in transcription and the presence of transcription factors [23–27], recently, the role of posttranscriptional regulation in T cells has also become appreciated [28–33]. Posttranscriptional regulation is mediated by sequence elements and structures present in both the 5′ and 3′ untranslated regions (UTRs) of mRNA molecules [34–37] and by nucleoside modifications, such as adenine methylation [38]. By facilitating the binding of RNA-binding proteins (RBPs), microRNAs, and long noncoding RNAs, these regulators combined determine the actual protein output of a cell [37].

One of these sequence elements are adenylate uridylate-rich elements (AREs). AREs are AUUUA pentamers present in multimers in the 3′UTR of mRNA molecules [39, 40]. Interestingly, many cytokine transcripts contain AREs [37, 39]. They function as binding hubs for RBPs and microRNAs [39–41]. Binding to AREs by these factors mediates mRNA stability, localization, and translation, which orchestrates the protein output [30, 41–44]. By deleting the 3′UTR AREs from cytokine mRNA, the protein production is decoupled from ARE-mediated posttranscriptional regulation [30, 43, 45]. We recently showed that AREs present in the *Ifng* 3′UTR dampen antitumoral responses in a murine melanoma model [46]. In fact, removal of AREs from the *Ifng* locus resulted in prolonged IFN-γ production in a tumor suppressive microenvironment, which translated into substantially delayed tumor outgrowth and prolonged survival [46].

The 3′UTR of IFN-γ is highly conserved between mice and men, in particular the region containing the AREs [30]. Therefore, we hypothesized that the regulation of IFN-γ production is also conserved. To unravel the posttranscriptional regulation of IFN-γ in primary human T cells, we removed a 160 bp region by CRISPR-Cas9 technology from the *IFNG* 3′UTR locus that contained all AREs sequences. Similar to murine *Ifng* [46], removal of AREs from the human *IFNG* locus (ARE-Del) results in increased IFN-γ production. Combining T cell receptor (TCR) gene transfer with ARE deletion in primary human T cells confirmed increased IFN-γ production by ARE-Del T cells in response to antigen expressing tumor cells. The ARE-mediated regulation of IFN-γ is thus conserved in human T cells.

Results

Deletion of AREs from the *IFNG* locus by CRISPR-Cas9

The human *IFNG* 3′UTR contains 5 AU-rich elements (AREs), defined as AUUUA (Fig. 1A, capital underlined sequences). To remove all five ARE sequences within the 3′UTR of the *IFNG* locus, we designed two CRISPR RNAs (crRNAs) (Fig. 1A, capital bold sequence). As a control, we included non-targeting crRNAs (control). PBMC-derived human primary T cells were activated with α-CD3/α-CD28 for 3 days prior to nucleofection with 30 μg Cas9 ribonuclear protein (RNP) complexes (Fig. 1B). Using ATTO550-labeled trans-activating CRISPR (tracr)RNA allowed us to follow the nucleofection efficiency by flow cytometry. Three days after nucleofection, virtually all $CD8^+$ and $CD4^+$ T cells were positive for ATTO550 (control 97.8 ± 0.9%, ARE-Del 98.6 ± 0.4%, Fig. 1C and D). In line with the described cleavage pattern of *S. pyogenes* Cas9 [47], cleavage occurred between the 17th and 18th base of the designed crRNAs (Supporting Information Fig. 2A). The 160 bp deletion containing the five AREs was efficient, as revealed by both PCR and Sanger sequencing of the genomic *IFNG* 3′UTR region (Fig. 1E; Supporting Information Fig. 2A). After experiencing cellular stress in the first 24 h, within 72 h, ARE-Del T and control T cells recovered and were viable (Fig. 1D). Furthermore, ARE-Del T and control T cells expanded 9.2 ± 1.1 fold and 8.9 ± 1.2 fold expansion within 8 days after removal from α-CD3/α-CD28, respectively.

To determine if gene editing affected the *IFNG* 3′UTR downstream of the ARE region, we extracted RNA from control and ARE-Del T cells. T cells were first activated for 3 h with α-CD3/α-CD28 to increase the expression of *IFNG* mRNA. After cDNA synthesis, we performed PCR from the end of the *IFNG* mRNA coding region to the 3′ end of the *IFNG* 3′UTR, resulting in a 509 bp fragment for the WT and a 349 bp fragment for the ARE-Del *IFNG* mRNA (Supporting Information Fig. 2B). The gene editing was thus specific for the ARE region and did not result in a premature transcriptional stop of the *IFNG* 3′UTR. In conclusion, ARE deletion from the *IFNG* locus was efficient in primary human T cells.

ARE deletion stabilizes *IFNG* mRNA and augments protein production in human T cells

We next studied whether ARE deletion from the *IFNG* locus altered *IFNG* mRNA levels. In T cells that were cultured for 9 days after nucleofection, *IFNG* mRNA levels were approximately twofold higher in ARE-Del T cells compared to control T cells (Fig. 2A). In most donors, *IFNG* mRNA levels of ARE-Del T cells were also slightly increased upon 3 h stimulation with α-CD3/α-CD28 compared to control T cells (Fig. 2A). *TNFA* and *IL2* mRNA levels remained unaltered, indicating *IFNG* mRNA-specific alterations in ARE-Del T cells (Supporting Information Fig. 3A). To measure the half-life of *IFNG* mRNA, we activated control and ARE-Del T cells for 3 h with α-CD3/α-CD28, and then blocked de novo mRNA transcription with actinomycin D [48]. ARE-deletion resulted in a significant increase of *IFNG* mRNA stability compared to control T cells ($t1/2 > 2$ h compared to ~70 min, Fig. 2B).

To determine whether ARE deletion also modulated the IFN-γ protein production and/or kinetics, we activated ARE-Del and control T cells with α-CD3/α-CD28. To visualize the IFN-γ production kinetics, we added brefeldin A for a maximum of the

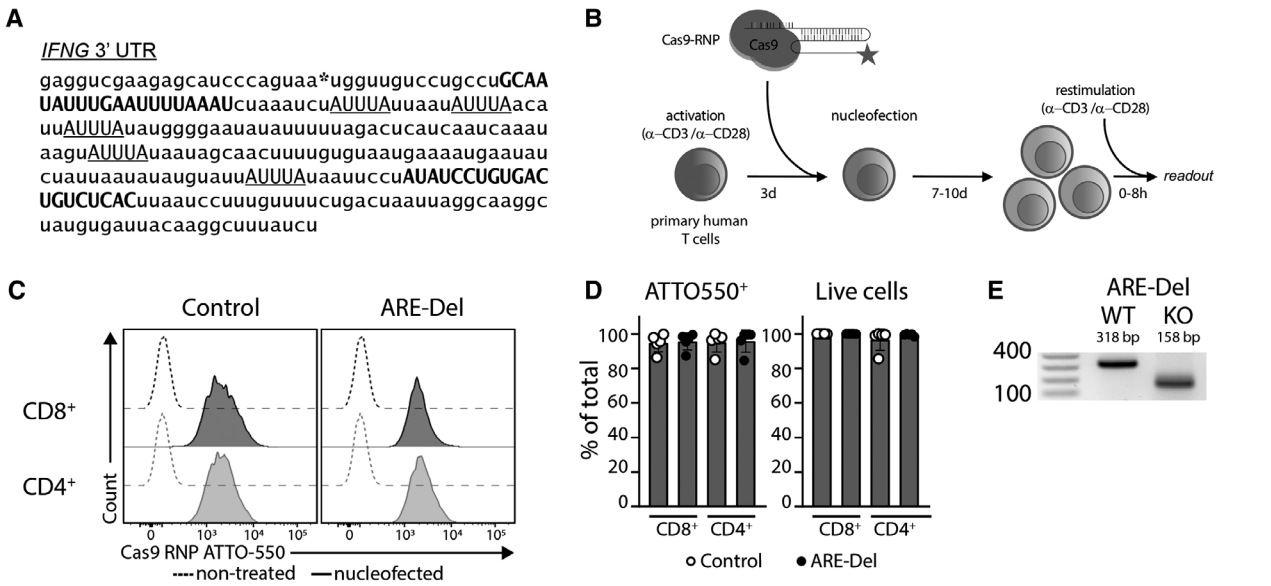

Figure 1. Generation of primary human ARE-Del T cells. (A) Sequence of the human *IFNG* 3′ UTR. Translation stop site is indicated with an asterisk, crRNA sequences are bold capitals, AREs are underlined capitals. (B) Graphical representation of the experimental setup. (C and D) PBMCs were stimulated for 72 h with α-CD3/α-CD28 and subsequently nucleofected with Cas9 RNPs with ATTO550-labeled crRNAs targeting the 3′UTR of *IFNG* (ARE-Del), or with non-targeting control crRNA (Control). (C) Representative flow cytometry histograms of Cas9 RNP-ATTO550 fluorescence gated on live $CD8^+$ T cells (black) and live $CD4^+$ T cells (gray). Dotted histograms represent non-nucleofected T cells. (D) Compiled flow cytometry data on ATTO550 fluorescence (left) and percentage of live cells (right) from $n = 5$ healthy donors from three independent experiments gated on $CD8^+$ and $CD4^+$ T cells, respectively. (E) ARE-deletion was analyzed by genomic PCR and subsequent gel analysis. Representative image of the control PCR performed for each donor in every experiment.

final 2 h of stimulation [49], and measured the production of IFN-γ protein by intracellular cytokine staining. In line with our previous findings in murine in vitro cultured ARE-Del T cells [30, 46], we did not detect IFN-γ protein production in human control or ARE-Del T cells unless the cells were reactivated with α-CD3/α-CD28 (Fig. 2C). Only after 2 h of activation, cytokine production was detectable and peaked at 6 h after stimulation in control and ARE-Del T cells (Fig. 2C), as previously described [3, 50]. However, already from 2 h of activation onwards, we found increased percentages of IFN-γ-producing T cells in ARE-Del $CD8^+$ T cells compared to control T cells (Fig. 2C and D). This increase in cytokine production was specific to IFN-γ and was not observed for tumor necrosis factor α (TNF-α) or interleukin 2 (IL-2, Supporting Information Fig. 3B and C). Even though we did not find overt differences in the IFN-γ production per cell (Fig. 2D, bottom row), deletion of AREs promoted the IFN-γ production in both $CD8^+$ and in $CD4^+$ T cells (Fig. 2D, top row). Thus, ARE deletion in the *IFNG* 3′UTR increases the stability of *IFNG* mRNA and augments the production of IFN-γ protein by human T cells.

Prolonged cytokine production by human ARE-Del T cells upon removal of stimuli

We next questioned if ARE deletion also modulates *IFNG* mRNA expression and protein production kinetics upon removal of stimulation. We restimulated ARE-Del T cells and control T cells with α-CD3/α-CD28 for 72 h and transferred the cells to new wells to remove the stimulus. Twenty-four hours after removing the T cells from the stimulus, control T cells expressed slightly lower *IFNG* mRNA levels than ARE-Del T cells, which further dropped after 48 h (Fig. 3A). In contrast, ARE-Del T cells maintained similarly high *IFNG* mRNA levels for up to 72 h after removal from stimulation (Fig. 3A).

We next measured the protein production after removal from stimuli. The production of TNF-α and IL-2 was lost in all T cells at 24 h after removal from stimulation (Supporting Information Fig. 3D). Control T cells and ARE-Del $CD8^+$ T cells also produced less IFN-γ protein at 24 h (Fig. 3B and C). However, in particular ARE-Del $CD8^+$ T cells showed low but sustained protein production of IFN-γ for up to 72 h (Fig. 3B and C). This also resulted in higher IFN-γ production per cell at 24 h after antigen removal, as determined by the GeoMFI of the IFN-γ producing T cells (Fig. 3C). The increased percentage of IFN-γ producing cells is also observed in $CD4^+$ ARE-Del T cells, albeit only for the first 24 h (Fig. 3C). Together, these data show that, similar to murine T cells [30], deletion of AREs from the *IFNG* 3′ UTR results in prolonged IFN-γ production in human T cells.

TCR-engineered ARE-Del T cells are superior IFN-γ producers in response to tumor cells

Finally, we questioned if and how the deletion of AREs in the *IFNG* gene affects antigen-specific T cell responses. To this end, we first tested whether CRISPR-Cas9-mediated ARE-Del deletion

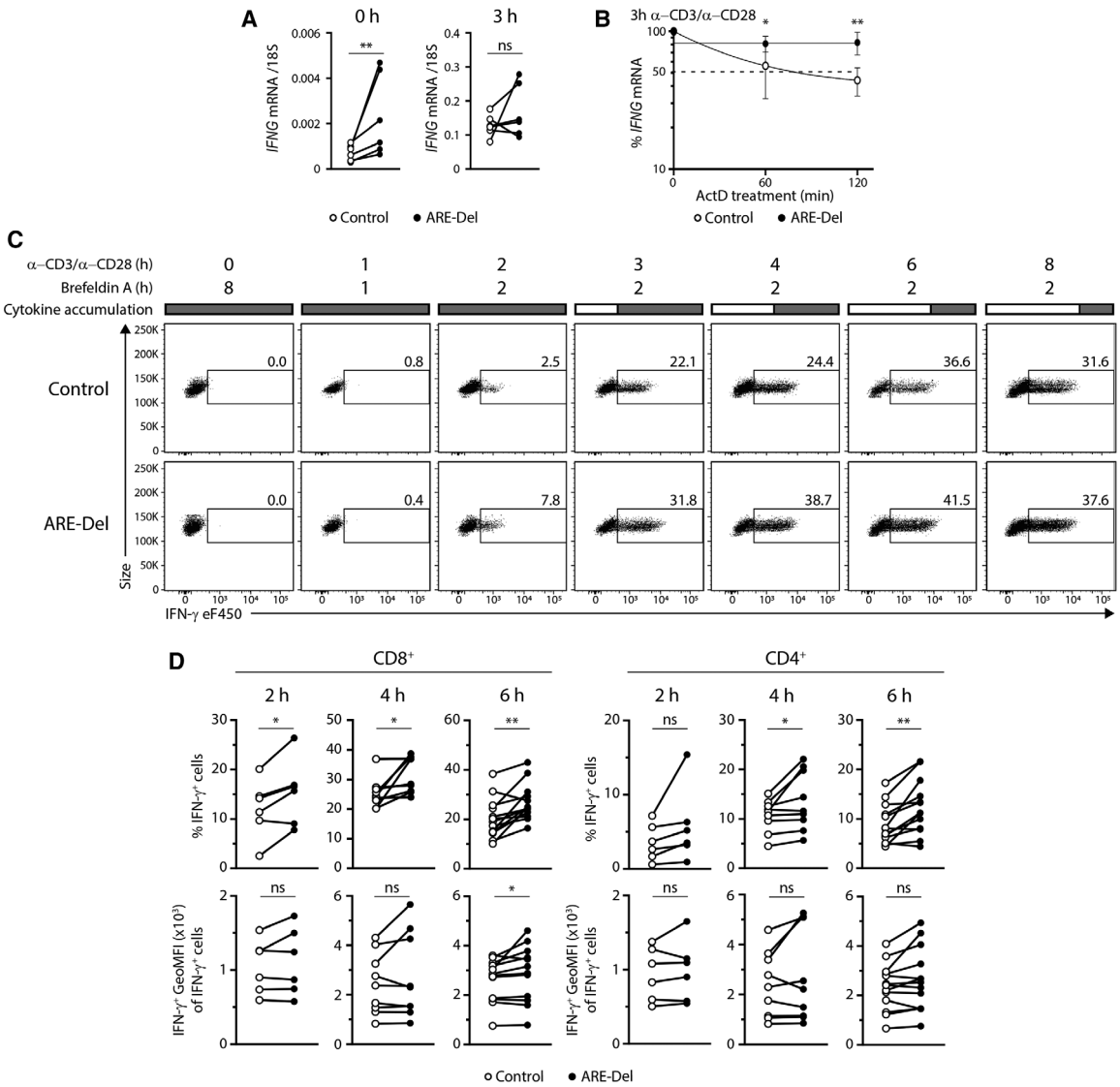

Figure 2. Enhanced *IFNG* mRNA levels, mRNA stability, and IFN-γ protein output in ARE-Del T cells. (A and B) T cells rested 9 days and were left untreated or restimulated for 3 h with α-CD3/α-CD28. (A) *IFNG* mRNA levels as determined by RT-PCR from $n = 6$ donors from two independent experiments (paired Student's *t*-test; $^{*}p < 0.05$, ns, not significant). (B) T cells were activated for 3 h with α-CD3/α-CD28. Actinomycin D was added to block de novo mRNA transcription, and *IFNG* mRNA stability was determined following 0, 60, and 120 min of actinomycin D treatment. $n = 4$ donors from two independent experiments (two-way ANOVA; $^{*}p < 0.05$, $^{**}p < 0.01$). (C and D) Resting T cells were restimulated with α-CD3/α-CD28 in the presence of brefeldin A for indicated time points. (C) Representative flow cytometry dot plots of IFN-γ production gated on live $CD8^+$ T cells. (D) Compiled flow cytometry data on IFN-γ^+ cells (top row) and IFN-γ GeoMFI (bottom row) gated on IFN-γ^+ $CD8^+$ and $CD4^+$ T cells from $n = 6$–13 donors from five to seven independent experiments after 2, 4 and 6 h of stimulation (paired Student's *t*-test; $^{*}p < 0.05$, $^{**}p < 0.01$, ns, not significant). Brefeldin A was added during the last 2 h of activation. T cells cultured in the absence of stimuli were used as negative control.

could be combined with TCR engineering. We first retrovirally transduced human $CD8^+$ T cells with a codon-optimized MART-1 TCR that recognizes the HLA-A*0201 restricted epitope of MART-1 (aa26-35) [51]. After 5 days, MART-1 TCR engineered T cells were restimulated with α-CD3/α-CD28 for 72 h prior to nucleofection. ARE deletion was also highly efficient in TCR-engineered T cells (Supporting Information Fig. 3E). Furthermore, the combined TCR engineering with subsequent nucleofection did not affect the viability or the expansion capacity of ARE-Del versus control MART-1 TCR-engineered T cells (92.3 ± 2.3 vs. 91.3 ± 2.6% of live cells at 48 h after nucleofection, and 12.9 ± 5.2 vs. 13.2 ± 4.2 fold expansion within 7 days, respectively).

To study the production of IFN-γ in response to target cells, we exposed MART-1 TCR-engineered ARE-Del T cells or control T cells to a MART-1^{hi} HLA-A*0201$^+$ melanoma cell line (MART-1^+), or to a MART-1^{lo} HLA-A*0201$^-$ melanoma cell line (MART-1^-) [52–54]. As expected, MART-1 TCR-engineered T cells only produce cytokines when co-cultured with MART-1^+ tumor cells (Fig. 4A). Also when T cell activation depended on cognate peptide-MHC complex, a significantly higher percentage of MART-1 TCR-engineered ARE-Del $CD8^+$ T cells produced

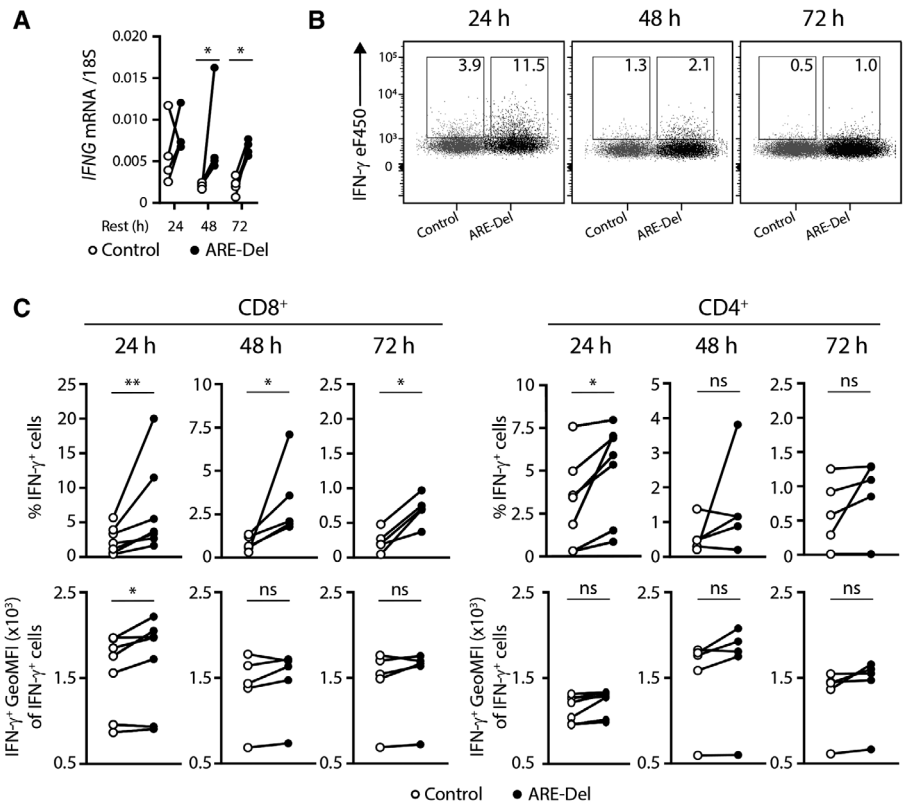

Figure 3. Prolonged IFN-γ production in ARE-Del T cells in the absence of stimulation. Rested T cells (11 days) were restimulated for 72 h with α-CD3/α-CD28 and removed from stimulus for indicated time. (A) *IFNG* mRNA levels as determined by RT-PCR from $n = 4$ donors from one experiment (paired Student's *t*-test; $^{*}p < 0.05$, ns, not significant). (B and C) IFN-γ protein production was assessed by adding brefeldin A 4 h prior to IFN-γ production assessment. (B) Representative concatenated flow cytometry dot plots of IFN-γ production of control and ARE-Del T cells after removal from stimulus for indicated time points. Separately measured samples containing control or ARE-Del T cells were gated on live $CD8^+$ T cells (as depicted in Supporting Information Fig. 1A), exported and subsequently concatenated into one dot plot. IFN-γ production is shown on the *y*-axis; samples are separated on the *x*-axis based on SampleID. Control T cells are depicted in gray, and ARE-Del T cells are depicted in black. (C) Compiled flow cytometry data on IFN-γ protein production from $n = 7$ donors from three independent experiments (ratio paired Student's *t*-test; $^{*}p < 0.05$, $^{**}p < 0.01$, ns, not significant).

IFN-γ after 6 h of co-culture with MART-1^+ cells than control MART-1 TCR-engineered T cells (Fig. 4A and B). Again, the higher percentage of IFN-γ producing ARE-Del T cells did not translate into significantly increased cytokine production per cell, as determined by the GeoMFI of the IFN-γ^+ T cells (Fig. 4B).

The percentage of IFN-γ producing cells was substantially reduced after 24 h of co-culture in both control and ARE-Del T cells, yet the percentage of IFN-γ–producing ARE-Del MART-1 TCR-engineered T cells was higher compared to control T cells (Fig. 4B). We also transferred the T cells to freshly seeded tumor cells for another 24 h. At this time point, that is, 48 h of co-culture, differences in cytokine production were lost (Fig. 4B). Overall, these finding show that the generation of antigen-specific ARE-Del T cells is feasible and that the ARE-deletion promotes the IFN-γ production in response to target cells.

Discussion

Here, we show that the deletion of AREs from the *IFNG* 3′UTR in primary human T cells results in higher *IFNG* mRNA levels, enhanced numbers of IFN-γ-producing T cells, and prolonged IFN-γ production. These findings are in line with previous findings with murine ARE-Del T cells [43, 46]. Since exogenously expressed GFP reporter genes containing a full-length *IFNG* 3′UTR variant with point mutations in all five AREs showed similar results in human T cells as ARE-Del T cells we generated here [30], we postulate that the observed enhanced IFN-γ production is at least in large part driven by the ARE deletion, and not merely a result of shortening the *IFNG* 3′UTR. Thus, the highly conserved ARE region in the *IFNG* 3′UTR locus also provides conserved posttranscriptional regulation in T cells.

Intriguingly, even though nonactivated murine memory T cells show leaky cytokine production directly ex vivo [30], this feature was not conserved in in vitro cultured T cells [30]. The lack of leaky cytokine production in the absence of stimulation is also observed in in vitro cultured human ARE-Del cells. This could either stem from leaky IFN-γ production levels that are below the detection limit, or from lack of additional signals that are required to off-set the protein production, and that are only present in vivo.

We also observed differences between murine and human ARE-Del T cells, which are primarily of quantitative nature. Murine ARE-Del T cells produce more IFN-γ per cell than WT T cells [46]. We did not observe this difference in human T cells. The overall mRNA stability in activated human control T cells is also lower than that of murine T cells. While WT murine T cells show a $t1/2 > 2$ h upon antigen stimulation [30, 33], human control T cells activated with α-CD3/α-CD28 only reach a $t1/2 \sim 70$ min. This also translates into lower overall IFN-γ protein output in human T cells, both in terms of responding T cells (60–80% in murine WT T cells versus 30–50% in human T cells upon PMA-Ionomycin stimulation [49, 50]), and in terms of production kinetics. In fact, even though human and murine T cells initiate the IFN-γ production at similar time points, human T cells cease to produce IFN-γ faster. To date, it remains unresolved whether these differences stem from different activation methods in murine and human T cells (MEF cells expressing antigen and B7.1 in murine [46] vs. α-CD3/α-CD28 in human T cells), from

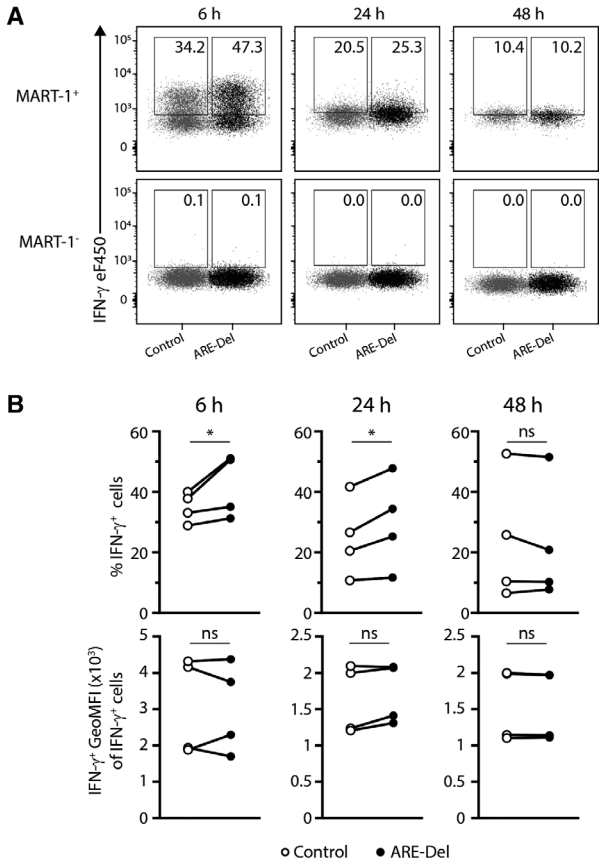

Figure 4. Enhanced IFN-γ production by ARE-Del T cells upon target cell recognition. MART-1 TCR-engineered T cells were co-cultured with MART-1$^+$ and MART-1$^-$ cell lines expressing MART-1 peptide for indicated time points. Brefeldin A was added 2 h prior to IFN-γ production assessment. To define IFN-γ producing T cells, MART-1 TCR$^+$ T cells co-cultured with MART-1$^-$ cells were used. Control T cells are depicted in gray, and ARE-Del T cells are depicted in black. (A) Representative concatenated flow cytometry dot plots of IFN-γ production of control and ARE-Del T cells after 6, 24, and 48 h of co-culture with MART-1$^+$ and MART-1$^-$ tumor cells. Separately measured samples containing control or ARE-Del T cells were gated on live CD8$^+$ T MART-1 TCR$^+$ T cells (as depicted in Supporting Information Fig. 1B), exported and subsequently concatenated into one dot plot. IFN-γ production is shown on the y-axis; samples are separated on the x-axis based on SampleID. Control T cells are depicted in gray, and ARE-Del T cells are depicted in black. (B) Compiled flow cytometry data from $n = 4$ donors from three independent experiments (paired Student's t-test; $^*p < 0.05$, ns, not significant).

different T cell responsiveness due to different requirements on nutrients and stimuli during culture conditions, from higher diversity in human CD8$^+$ T cell populations [55], or from intrinsic differences between murine and human T cells. Irrespective of the observed quantitative differences, we show here that ARE sequences are essential for the regulation of *IFNG* mRNA stability and IFN-γ protein output in both murine [46] and human T cells.

ARE-mediated regulation of mRNA transcripts depends at least in part on mRNA binding of RBPs [37]. Which ARE-binding proteins regulate the production of IFN-γ in activated human T cells remains to be determined. Our laboratory previously reported that the ARE-binding protein Zfp36l2 blocks the translation of preformed *Ifng* mRNA in murine memory T cells [30]. Zfp36l2, however, releases *Ifng* mRNA upon reactivation, allowing T cells to instantaneously produce IFN-γ from this preformed mRNA [30, 49]. Because *Ifng* mRNA is released from Zfp36l2 upon murine T cell activation, we consider it unlikely that this RBP drives ARE-mediated posttranscriptional events in activated human T cells, at least in the early phase of T cell activation. Other possible candidates to modulate the fate of *IFNG* mRNA are the family members of ZFP36L2, that is, ZFP36 and ZFP36L1 [56]. Their potential contribution in regulating the production of IFN-γ in human T cells is, however, yet to be experimentally addressed.

Excessive production of IFN-γ can induce immunopathology [57–65]. However, the AREs solely fine-tune posttranscriptional regulation of IFN-γ production, while leaving the requirement of antigen recognition and transcriptional regulation in murine and human T cells intact ([46], this study). Indeed, in studies with long-term memory ARE-Del T cells in a *Listeria monocytogenes* infection and in a B16 melanoma model, we find the increased and prolonged IFN-γ production only in the presence of tumor cells or after antigenic challenge [46]. We therefore anticipate only limited side effects of the ARE deletion in T cells.

We here combined retroviral TCR engineering with efficient CRISPR-Cas9-mediated genome editing. This experimental setup is a powerful tool to study gene modification in human T cells in an antigen-specific setting. Furthermore, TCR engineering with CRISPR-Cas9 technology could also be useful for therapeutic purposes. IFN-γ-mediated signaling is key for effective antitumoral T cell responses and immunotherapy efficiency [19–21, 66]. Currently, several different types of cancer are treated with genetically engineered T cells that express a CAR against leukemic antigens like CD19 [67], or a TCR that is specific for a tumor (neo)antigen [68–70]. It is therefore tempting to speculate that modifying genetically engineered T cell products with an additional *IFNG* ARE deletion could help maintaining their potential to specifically produce more IFN-γ in the tumor environment and thus help increase their antitumoral potential. It is noteworthy that upon CRISPR-Cas9-mediated genome editing, TCR-engineered T cells maintained their capacity to expand, a feature that is critical for generating the large numbers of T cells required for cellular products.

In conclusion, the generation of primary human ARE-Del T cells revealed that fundamental posttranscriptional mechanisms of *IFNG* regulation are conserved throughout evolution.

Materials and methods

Human PBMCs and cell culture

Studies with human T cells from anonymized healthy donors were performed in accordance with the Declaration of Helsinki (Seventh Revision, 2013) after written informed consent (Sanquin). Peripheral blood mononuclear cells (PBMCs) were isolated through Lymphoprep density gradient separation (Stemcell Technologies). Cells were used after cryopreservation.

Table 1. Primers used in this study

Name	Sequence (5′→3′)
ARE-Del gRNA 1	GTGAGACAGTCACAGGATAT
ARE-Del gRNA 2	ATTTAAAATTCAAATATTGC
ARE-Del PCR F	TCGAGGTCGAAGAGCATCCC
ARE-Del PCR R	CCCATGGGATCTTGCTTAGGT
IFNG_3′PCR_F	TCGAGGTCGAAGAGCATCCC
IFNG_3′PCR_R	GGAAGCACCAGGCATGAAATC

Human T cells were cultured in T cell mixed media (Miltenyi) supplemented with 5% heat-inactivated human AB0 serum (Sanquin) and fetal bovine serum (FBS; Bodinco), 2 mM L-glutamine, 20 IU/mL penicillin G sodium salts, 20 μg/mL streptomycin sulfate (all Sigma Aldrich), 100 IU/mL recombinant human (rh) IL-2 (Proleukin, Novartis), and 10 ng/mL rhIL-15 (Peprotech), and were cultured in a humidified incubator at 37°C + 5% CO_2. Cells were cultured at a density between 0.5 and 1 × 10^6 cells/mL. Medium was refreshed every 3 days.

T cell activation

T cells were activated as previously described [50]. Briefly, 24-well plates were precoated overnight with 0.5 μg/mL rat α-mouse IgG2a (clone MW1483; Sanquin) at 4°C. Plates were washed once with PBS, coated with 1 μg/mL α−CD3 (clone Hit3a, eBioscience) for a minimum of 2 h at 37°C, and washed once with PBS. 1 × 10^6 PBMCs/well were added in medium supplemented with 1 μg/mL α-CD28 (clone CD28.2; eBioscience). Cells were activated for 72 h in a humidified incubator at 37°C and 5% CO_2.

crRNA and sequence primer design

crRNAs and sequence primers were designed using the CRISPR and Primer design tools in Benchling (https://benchling.com, Table 1). Sequences were verified to be specific for the target of interest via BlastN and PrimerBlast (both NCBI).

Genetic modification of human T cells with Cas9-RNPs

Cas9 RNP production and T cell nucleofection was performed as previously described [71]. Briefly, Alt-R crRNA and ATTO550-labeled tracr-RNA were reconstituted to 100 μM in Nuclease Free Duplex buffer (all Integrated DNA Technologies). As a negative control, non-targeting negative control crRNA #1 was used (Integrated DNA Technologies). Oligos were mixed at equimolar ratios (i.e., 4.5 μL total crRNA + 4.5 μL transactivating CRISPR RNA) in nuclease-free PCR tubes and denatured by heating at 95°C for 5 min in a thermocycler. Nucleic acids were cooled down to room temperature prior to mixing them via pipetting with 30 μg TrueCut Cas9 V2 (Invitrogen) to produce Cas9 RNPs. Mixture was incubated at room temperature for at least 10 min prior to nucleofection.

For nucleofection, 1 × 10^6 T cells/condition were harvested 72 h after α-CD3/α-CD28 activation and transferred to DNA Lobinding Eppendorf tubes (Eppendorf). Cells were washed once with PBS and supernatant was completely removed. Cells were resuspended in 20 μL P2 Buffer (Lonza), Cas9 RNPs were added, and incubated for 2 min. Cells were then electroporated in 16-well strips in a 4D Nucleofector X unit (Lonza) with program EH-100. 100 μL of prewarmed complete medium was added after nucleofection and cells were allowed to recover for 5 min in a humidified incubator at 37°C and 5% CO_2. Cells were transferred to 48-well plates containing 500 μL prewarmed complete medium and cultured in a humidified incubator at 37°C + 5% CO_2.

CRISPR-mediated gene editing was tested on genomic DNA. Snapfrozen cell pellets (1 × 10^6 cells) were incubated overnight at 56°C, while rotating at 850 RPM in 50 μL lysis buffer (50 mM Tris-HCl, 2.5 mM EDTA, 50 mM KCl, and 0.45% Tergitol at pH 8.0) that was freshly supplemented with 1 μg/mL proteinase K (Roche). After deactivating proteinase K by incubating for 15 min at 95°C, lysed cells were centrifuged for 10 min at 13 000 RPM (20 000*g*). Supernatant was transferred to a new tube. The *IFNG* genomic locus was amplified by PCR (30 s at 98°C, (10 s at 98°C, 30 s at 65°C, 30 s at 72°C) × 40, 7 min at 72°C, 2 min at 15°C) with DreamTaq HotStart Green Polymerase (ThermoScientific) and primerpair ARE-Del_PCR_F and ARE-Del_PCR_R (Table 1) and subsequently analyzed on 0.8% agarose gel. For Sanger sequencing, PCR product was purified with NucleoSpin Gel and PCR Clean-up kit (Macherey Nagel) according to manufacturer's protocol (Baseclear).

ARE deletion from *IFNG* mRNA was determined by total RNA extraction from snapfrozen pellets of 0.2 × 10^6 cells activated for 3 h with α-CD3/α-CD28-activated T cells using Trizol (Invitrogen). DNA contamination was removed with RNA Clean & Concentrator 5 kit (Zymo Research) according to manufacturer's protocol. cDNA synthesis was performed in the presence or absence of SuperScript III Reverse Transcriptase according to manufacturer's protocol (Invitrogen). The resulting cDNA was amplified by PCR (30 s at 98°C, (10 s at 98°C, 30 s at 62°C, 30 s at 72°C) × 40, 7 min at 72°C, 2 min at 15°C) with DreamTaq HotStart Green Polymerase and primerpair IFNG_3′PCR_F and IFNG_3′PCR_R (Table 1) and subsequently analyzed on a 2% agarose gel.

Generation of MART-1 TCR expressing T cells

PBMCs were activated for 72 h with α-CD3/α-CD28, harvested, and transduced with MART-1 TCR retrovirus as previously described [51]. Briefly, nontissue culture treated 24-well plates were coated with 50 μg/mL Retronectin (Takara) overnight at 4°C and washed once with PBS. Subsequently, 300 μL viral supernatant was added per well and was centrifuged for 1 h at 4°C at 4000 rpm (2820*g*). Note that 1 × 10^6 freshly activated T cells were added per well, spun for 10 min at 1000 rpm (180*g*), and cultured at 37°C and 5% CO_2 in a humidified incubator. After 24 h, cells were harvested and cultured in T25 flasks at a concentration of 0.8 × 10^6 cells/mL for 3 days in complete medium.

Functional assays

T cells were stimulated with 1 μg/mL precoated α-CD3 and 1 μg/mL soluble α-CD28 for indicated time points. MART-1 TCR-transduced T cells were co-cultured with HLA-A*0201$^+$ MART1^{hi} Mel 526 (MART1$^+$), or HLA-A*0201$^-$ MART1^{lo} Mel 888 (MART1$^-$) tumor cell lines [52–54], in a 1:1 effector to target (E:T) ratio for indicated time points. 1 μg/mL brefeldin A (BD Biosciences) was added as indicated. Nonactivated T cells were used as a negative control. All stimulations were performed in T cell mixed medium supplemented with 10% FBS, 2 mM L-glutamine, 20 U/mL penicillin G sodium salts, and 20 μg/mL streptomycin sulfate.

Flow cytometry and intracellular cytokine staining

For flow cytometric analysis, cells were washed with FACS buffer (PBS, containing 1% FBS and 2 mM EDTA) and labeled with monoclonal antibodies α-CD4 (clone SK3), α-CD8 (clone SK1), α-murine TCR beta (clone H57-597; all BD Biosciences), α-IFN-γ (clone 4S.B3), α-IL-2 (clone MQ1-17H12), and α-TNF-α (clone MAb11) (all Biolegend). Near-IR (Life Technologies) was used to exclude dead cells from analysis. For intracellular cytokine staining, cells were cultured in the presence of 1 μg/mL brefeldin A for indicated time points and were fixed and permeabilized with Cytofix/Cytoperm kit (BD Biosciences) according to manufacturer's protocol. Expression levels were acquired using FACSymphony (BD Biosciences) and data were analyzed using FlowJo (FlowJo LLC, version 10). For gating strategy, see Supporting Information Fig. 1A and B. The guidelines for the use of flow cytometry and cell sorting in immunological studies [72] were followed as noted in sections III.1–5 of ref. [72].

Real-time PCR analysis

Total RNA was extracted using Trizol (Invitrogen). cDNA synthesis was performed with SuperScript III Reverse Transcriptase (Invitrogen), and real-time PCR was performed with SYBR Green and a StepOne Plus RT-PCR system (both Applied Biosystems). Reactions were performed in duplicate or triplicate, and cycle threshold values were normalized to *18S* levels. Primer sequences for *IFNG, TNF*, and *IL2* mRNA were previously described [50].

To determine the $t_{1/2}$ of *IFNG* mRNA, T cells were activated for 3 h with indicated stimuli, and then treated with 5 μg/mL actinomycin D (ActD) (Sigma-Aldrich). Data were analyzed using StepOne Plus software (Applied Biosystems).

Statistical analysis

Results are expressed as mean ± SD when indicated. Statistical analysis between groups was performed with Prism (GraphPad Software, version 8), using paired or ratio-paired Student's *t*-test when comparing two groups as indicated, or two-way ANOVA with Bonferroni's correction for multiple comparisons when comparing more than two groups. p values < 0.05 were considered to be statistically significant.

Acknowledgements: This research was supported by KWF Kankerbestrijding (10132), the Dutch Science Foundation (VIDI grant 917.14.214), and Oncode Institute (all to M.C.W).

Author Contributions: J.J.F.H., B.P., and M.C.W. designed experiments; J.J.F.H., B.P., and A.G. performed experiments; J.J.F.H., B.P., and M.C.W. analyzed data; and J.J.F.H. and M.C.W. wrote the manuscript. M.C.W. supervised the project.

The authors would like to thank Dr. Ton Schumacher (Netherlands Cancer Institute) for providing MART-1 TCR viral supernatants, Nordin Zandhuis for technical assistance, and the Wolkers' lab for scientific input and critical reading of the manuscript.

Conflict of interest: The authors declare no financial or commercial conflict of interest.

References

1 **Almeida, J. R., Price, D. A., Papagno, L., Sauce, D., Bornstein, E., Asher, T. E., Samri, A. et al.**, Superior control of HIV-1 replication by CD8$^+$ T cells is reflected by their avidity, polyfunctionality, and clonal turnover. *J. Exp. Med.* 2007; **204**: 2473–2485.

2 **Ciuffreda, D., Comte, D., Cavassini, M., Giostra, E., Bu, L., Perruchoud, M., Heim, M. H. et al.**, Polyfunctional HCV-specific T-cell responses are associated with effective control of HCV replication. *Eur. J. Immunol.* 2008; **38**: 2665–2677.

3 **Han, Q., Bagheri, N., Bradshaw, E. M., Hafler, D. A., Lauffenburger, D. A. and Love, J. C.**, Polyfunctional responses by human T cells result from sequential release of cytokines. *Proc. Natl. Acad. Sci. USA* 2012; **109**:1607–1612.

4 **Beatty, G. L. and Paterson, Y.** IFN-γ-dependent inhibition of tumor angiogenesis by tumor-infiltrating CD4$^+$ T cells requires tumor responsiveness to IFN-γ. *J. Immunol.* 2001; **166**: 2276–2282.

5 **Schroder, K., Hertzog, P. J., Ravasi, T. and Hume, D. A.** Interferon-gamma: an overview of signals, mechanisms and functions. *J. Leukoc. Biol.* 2004; **75**: 163–89.

6 **Libregts, S. F., Gutie, L., De, B. A.M., Wensveen, F. M., Papadopoulos, P., Van, I. W., Zeliha, O. et al.**, Chronic IFN-γ production in mice induces anemia by reducing erythrocyte life span and inhibiting erythropoiesis through an IRF-1/PU.1 axis. *Blood* 2011; **118**: 2578–2589.

7 **De Bruin, A. M., Voermans, C. and Nolte, M. A.**, Impact of interferon-γ on hematopoiesis. *Blood* 2014; **124**: 2479–2486.

8 **Ching, L. F. and HA, Y.** Interferons: success in anti-viral immunotherapy. *Cytokine Growth Factor Rev.* 2014; **25**: 369–376.

9 **Soudja, S., Chandrabos, C., Yakob, E., Veenstra, M., Palliser, D. and Lauvau, G.**, Memory-T-cell-derived interferon-γ instructs potent innate cell activation for protective immunity. *Immunity* 2014; **40**: 974–968.

10 **Selders, G. S., Fetz, A. E., Radic, M. Z. and Bowlin, G. L.**, An overview of the role of neutrophils in innate immunity, inflammation and host-biomaterial integration. *Regen. Biomater.* 2017:55–68.

11 **Nathan, C., Murray, H., Wiebe, M. and Rubin, B.**, Identification of interferon-gamma as the lymphokine that activates human macrophage oxidative metabolism and antimicrobial activity. *J. Exp. Med.* 1983; **158**: 670–689.

12 **Martinez, F. O., Helming, L. and Gordon, S.**, Alternative activation of macrophages: an immunologic functional perspective. *Annu. Rev. Immunol.* 2009; **27**: 451–483.

13 **Li, C., Xu, M. M., Wang, K., Adler, A. J., Vella, A. T. and Zhou, B.**, Macrophage polarization and metainflammation. *Transl. Res.* 2018; **191**: 29–44.

14 **Newport, M., Huxley, C., Huston, S., Hawrylowicz, C., Oostra, B., Williamson, R. and Levin, M.**, A mutation in the interferon-γ-receptor gene and susceptibility to mycobacterial infection. *N. Engl. J. Med.* 1996; **355**: 1941–1949.

15 **Dorman, S. E. and Holland, S M.**, Mutation in the signal-transducing chain of the interferon-γ receptor and susceptibility to mycobacterial infection. *J. Clin. Invest.* 1998; **101**: 2364–2369.

16 **Zhang, S., Chapgier, A., Yang, K., Bustamante, J., Puel, A., Picard, C., Abel, L. et al.**, Inborn errors of interferon (IFN)-mediated immunity in humans insights into the respective roles of IFN-a/b, IFN-g and IFN-d in host defense. *Immunol. Rev.* 2008; **276**: 29–40.

17 **Kaplan, D. H., Shankaran, V., Dighe, A. S., Stockert, E., Aguet, M., Old, L. J. and Schreiber, R. D.**, Demonstration of an interferon-gamma dependent tumor surveillance system in immunocompetent mice. *Proc. Natl. Acad. Sci. USA* 1998; **95**: 7556–7561.

18 **Shankaran, V., Ikeda, H., Bruce, A. T., White, J. M., Swanson, P. E., Old, L. J. and Schreiber, R. D.**, IFN-γ and lymphocytes prevent primary tumour development and shape tumour immunogenicity. *Nature* 2001; **410**: 1107–1111.

19 **Patel, S. J., Sanjana, N. E., Kishton, R. J., Eidizadeh, A., Vodnala, S. K., Cam, M. and Gartner, J. J. et al.**, Identification of essential genes for cancer immunotherapy. *Nature* 2017; **548**: 537–542.

20 **Ayers, M., Lunceford, J., Nebozhyn, M., Murphy, E., Loboda, A., Kaufman, D. R., Albright, A. et al.**, IFN-γ–related mRNA profile predicts clinical response to PD-1 blockade. *J. Clin. Invest.* 2017; **127**: 2930–2940.

21 **Gao, J., Shi, L. Z., Zhao, H., Chen, J., Xiong, L., He, Q., Chen, T. et al.**, Loss of IFN-γ pathway genes in tumor cells as a mechanism of resistance to anti-CTLA-4 therapy. *Cell* 2016; **167**: 397–404.

22 **Jones, B. and Chen, J.** Inhibition of IFN-gamma transcription by site-specific methylation during T helper cell development. *EMBO J.* 2006; **25**: 2443–2452.

23 **Sica, A., Dorman, L., Viggiano, V., Cippitelli, M., Ghosh, P., Rice, N. and Young, H. A.**, Interaction of NF-kB and NFAT with the interferon-γ promoter. *J. Biol. Chem.* 1997; **272**: 30412–30420.

24 **Intlekofer, A. M., Takemoto, N., Wherry, E. J., Longworth, S. A., Northrup, J. T., Palanivel, V. R., Mullen, A. C. et al.**, Effector and memory $CD8^+$ T cell fate coupled by T-bet and eomesodermin. *Nat. Immunol.* 2005; **6**: 1236–1244.

25 **Koch, A., Raidl, M., Lux, M. and Mu, K.**, IL-12-induced T-bet expression and IFN-γ release in lymphocytes from asthmatics—role of MAPkinases ERK-1/-2, p38 MAPK and effect of dexamethasone. *Respitory Med.* 2007; **101**: 1321–1330.

26 **Gray, S. M., Kaech, S. M. and Staron, M. M.**, The interface between transcriptional and epigenetic control of effector and memory. *Immunol. Rev.* 2014; **261**: 157–168.

27 **Conley, J. M., Gallagher, M. P. and Berg, L. J.**, T cells and gene regulation: the switching on and turning up of genes after T cell receptor stimulation in CD8 T cells. *Front. Immunol.* 2016; **7**: 76.

28 **Ganguly, K., Giddaluru, J., August, A. and Khan, N.**, Post-transcriptional regulation of immunological responses through riboclustering. *Front. Immunol.* 2016; **7**: 161.

29 **Hoefig, K. P. and Heissmeyer, V.** Posttranscriptional regulation of T helper cell fate decisions. *J. Cell Biol.* 2018; **217**: 2615–2631.

30 **Salerno, F., Engels, S., van den Biggelaar, M., Van Alphen, F. P. J., Guislain, A., Zhao, W., Hodge, D. L. et al.**, Translational repression of pre-formed cytokine-encoding mRNA prevents chronic activation of memory T cells. *Nat. Immunol.* 2018; **19**: 828–837.

31 **Turner, M. and Díaz-Muñoz, M D.**, RNA-binding proteins control gene expression and cell fate in the immune system. *Nat. Immunol.* 2018; **19**: 120–129.

32 **Gagnon, J. D., Kageyama, R., Shehata, H. M., Fassett, M. S., Mar, D. J., Wigton, E. J., Johansson, K. et al.**, miR-15/16 restrain memory T cell differentiation, cell cycle, and survival. *Cell Rep.* 2019; **28**: 2169–2181.

33 **Salerno, F., Freen-van Heeren, J. J., Guislain, A., Nicolet, B. P. and Wolkers, M. C.**, Costimulation through TLR2 drives polyfunctional $CD8^+$ T cell responses. *J. Immunol.* 2019; **202**: 714–723.

34 **Cohen-Chalamish, S., Hasson, A., Weinberg, D., Namer, L. S., Banai, Y., Osman, F. and Kaempfer, R.**, Dynamic refolding of IFN-gamma mRNA enables it to function as PKR activator and translation template. *Nat. Chem. Biol.* 2009; **5**:896–903.

35 **Kafasla, P., Skliris, A. and Kontoyiannis, D. L.**, Post-transcriptional coordination of immunological responses by RNA-binding proteins. *Nat. Immunol.* 2014; **15**: 492–502.

36 **Turner, M., Galloway, A. and Vigorito, E.**, Noncoding RNA and its associated proteins as regulatory elements of the immune system. *Nat. Immunol.* 2014; **15**: 484–491.

37 **Salerno, F. and Wolkers, M C.**, T-cells require post-transcriptional regulation for accurate immune responses. *Biochem. Soc. Trans.* 2015; **43**: 1201–1207.

38 **Yue, Y., Liu, J. and He, C.**, RNA N6-methyladenosine methylation in post-transcriptional gene expression regulation. *Genes Dev.* 2015; **29**: 1343–1355.

39 **Barreau, C., Paillard, L. and Osborne, H. B.**, AU-rich elements and associated factors: are there unifying principles? *Nucleic Acids Res.* 2005; **33**: 7138–50.

40 **Beisang, D. and Bohjanen, P.**, Perspectives on the ARE as it turns 25 years old. *Wiley Interdiscip Rev RNA.* 2012; **3**: 719–731.

41 **Jing, Q., Huang, S., Guth, S., Zarubin, T., Motoyama, A., Chen, J., Di Padova, F. et al.**, Involvement of microRNA in AU-rich element-mediated mRNA instability. *Cell* 2005; **120**: 623–634.

42 **Stoecklin, G., Lu, M., Rattenbacher, B. and Moroni, C.**, A constitutive decay element promotes tumor necrosis factor alpha mRNA degradation via an AU-rich element-independent pathway. *Mol. Cell. Biol.* 2003; **23**: 3506–15.

43 **Hodge, D. L., Berthet, C., Coppola, V., Kastenmüller, W., Buschman, M. D., Schaughency, P. M., Shirota, H. et al.**, IFN-gamma AU-rich element removal promotes chronic IFN-gamma expression and autoimmunity in mice. *J. Autoimmun.* 2014; **53**: 33–45.

44 **Vlasova-St. Louis, I. and Bohjanen, P. R.**, Post-transcriptional regulation of cytokine signaling by AU-rich and GU-rich elements. *J. Interf. Cytokine Res.* 2014; **34**: 233–241.

45 **Kontoyiannis, D., Pasparakis, M., Pizarro, T. T., Cominelli, F. and Kollias, G.**, Impaired on/off regulation of TNF biosynthesis in mice lacking TNF AU-rich elements: implications for joint and gut-associated immunopathologies. *Immunity* 1999; **10**: 387–398.

46 **Salerno, F., Guislain, A., Freen-van Heeren, J. J., Benoit, P., Young, H. A. and Wolkers, M. C.**, Critical role of post-transcriptional regulation for IFN-γ in tumor-infiltrating T cells. *Oncoimmunology*. 2018; **8**: e1532762.

47 **Jinek, M., Chylinski, K., Fonfara, I., Hauer, M., Doudna, J. A. and Charpentier, E.**, A programmable dual-RNA-guided DNA endonuclease in adaptive bacterial immunity. *Science* 2012; **337**: 816–821.

48 **Salerno, F., Guislain, A., Cansever, D. and Wolkers, M. C.**, TLR-mediated innate production of IFN-γ by $CD8^+$ T cells is independent of glycolysis. *J. Immunol.* 2016; **196**: 3695–3705.

49 **Salerno, F., Paolini, N. A., Stark, R., von Lindern, M. and Wolkers, M. C.**, Distinct PKC-mediated posttranscriptional events set cytokine production kinetics in $CD8^+$ T cells. *Proc. Natl. Acad. Sci. USA* 2017; **114**: 9677–9682.

50 **Nicolet, B. P., Guislain, A., Wolkers, M. C.**, Combined single-cell measurement of cytokine mRNA and protein identifies T cells with persistent effector function. *J. Immunol.* 2017; **198**: 962–970.

51 **Gomez-Eerland, R., Nuijen, B., Heemskerk, B., van Rooij, N., van den Berg, J. H., Beijnen, J. H., Uckert, W. et al.**, Manufacture of gene-modified human T-cells with a memory stem/central memory phenotype. *Hum. Gene Ther. Methods*. 2014; **25**: 277–287.

52 **Topalian, S. L., Solomon, D. and Rosenberg, S. A.**, Tumor-specific cytolysis by lymphocytes infiltrating human melanomas. *J. Immunol.* 1989; **142**: 3714–3725.

53 **Marincola, F. M., Shamamian, P., Simonis, T. B., Abati, A., Dea, T. O., Fetsch, P., Yannelli, J. et al.**, Locus-specific analysis of human leukocyte antigen class I expression in melanoma cell lines. *J. Immunother. Emphasis Tumor Immunol.* 1994; **16**: 13–23.

54 **Cormier, J. N., Panelli, M. C., Hackett, J. A., Bettinotti, M. P., Wunderlich, J., Parker, L. L., Restifo, N. P. et al.**, Natural variation of the expression of HLA and endogenous antigen modulates CTL recognition in an in vitro melanoma model. *Int. J. Cancer*. 1999; **80**: 781–790.

55 **Nicolet, B. P., Guislain, A., van Alphen, F. P. J., Gomez-Eerland, R., Schumacher, T. N., van den Biggelaar, M. and Wolkers, M.**, CD29 identifies IFN-g producing T cells human $CD8^+$ T cells with an increased cytotoxic potential. *Proc. Natl. Acad. Sci. USA*. 2020. In press. https://doi.org/10.1073/pnas.1913940117.

56 **Moore, M. J., Blachere, N. E., Fak, J. J., Park, C. Y., Sawicka, K., Parveen, S., Zucker-scharff, I. et al.**, ZFP36 RNA-binding proteins restrain T cell activation and anti-viral immunity. *Elife* 2018; **7**: e33057.

57 **Ito, R., Shin-Ya, M., Kishida, T., Urano, A., Takada, R., Sakagami, J., Imanishi, J. et al.**, Interferon-γ is causatively involved in experimental inflammatory bowel disease in mice. *Clin. Exp. Immunol.* 2006; **146**: 330–338.

58 **Rafa, H., Amri, M., Saoula, H., Belkhelfa, M., Medjeber, O. and Boutaleb, A.**, Involvement of interferon-γ in bowel disease pathogenesis by nitric oxide pathway: a study in Algerian patients. *J. Interf. Cytokine Res.* 2010; **30**: 691–697.

59 **Arellano, G., Ottum, P. A., Reyes, L. I., Burgos, P. I.**, Stage-specific role of interferon-γ in experimental autoimmune encephalomyelitis and multiple sclerosis. *Front. Immunol.* 2015; **6**: 492.

60 **Ostler, T., Davidson, W. and Ehl, S.**, Virus clearance and immunopathology by $CD8^+$ T cells during infection with respiratory syncytial virus are mediated by IFN-γ. *Eur. J. Immunol.* 2002; **32**: 2117–2123.

61 **Badovinac, V. P., Hamilton, S. E. and Harty, J. T.**, Viral infection results in massive $CD8^+$ T cell expansion and mortality in vaccinated perforin-deficient mice. *Immunity* 2003; **18**: 463–474.

62 **Kuphal, S., Bosserhoff, A.** Interferon-gamma-dependent mechanisms of mycobacteria-induced pulmonary immunopathology: the role of angiostasis and CXCR3-targeted chemokines for granuloma necrosis. *J. Pathol.* 2007; **212**: 295–305.

63 **Beccaria, C. G., Vesely, M. C. A., Vernengo, F. F., Gehrau, R. C., Ramello, M. C., Boari, J. T., Serrán, M. G. et al.**, Galectin-3 deficiency drives lupus-like disease by promoting spontaneous germinal centers formation via IFN-γ. *Nat. Commun.* 2018; **9**: 1628.

64 **Ivashkiv, L. B.**, IFNγ: signalling, epigenetics and roles in immunity, metabolism, disease and cancer immunotherapy. *Nat. Rev. Immunol.* 2018; **18**: 545–558.

65 **Lounder, D. T., Bin, Q., de Min, C. and Jordan, M. B.**, Treatment of refractory hemophagocytic lymphohistiocytosis with emapalumab despite severe concurrent infections. *Blood Adv.* 2019; **3**: 47–50.

66 **Alspach, E., Lussier, D. M. and Schreiber, R. D.**, Interferon γ and its important roles in promoting cancer immunity. *Cold Spring Harb. Perspect. Biol.* 2019; **11**: a028480.

67 **June, C. H. and Sadelain, M.**, Chimeric antigen receptor therapy. *N. Engl. J. Med.* 2018; **379**: 64–73.

68 **Bailey, S. R. and Maus M, V.**, Gene editing for immune cell therapies. *Nat. Biotechnol.* 2019; **37**: 1425–1434.

69 **Schumacher, T. N., Scheper, W. and Kvistborg, P.**, Cancer neoantigens. *Annu. Rev. Immunol.* 2019; **37**: 173–200.

70 **Yamamoto, T. N., Kishton, R. J. and Restifo, N. P.**, Developing neoantigen-targeted T cell–based treatments for solid tumors. *Nat. Med.* 2019; **25**: 1488–1499.

71 **Seki, A. and Rutz, S.** Optimized RNP transfection for highly efficient CRISPR/Cas9-mediated gene knockout in primary T cells. *J. Exp. Med.* 2018; **215**: 985–997.

72 **Cossarizza, A., Chang, H. D., Radbruch, A., Acs, A., Adam, D., Adam-Klages, S., Agace, W. W. et al.**, Guidelines for the use of flow cytometry and cell sorting in immunological studies (second edition). *Eur. J. Immunol.* 2019; **49**: 1457–1973.

Abbreviations: **ARE**: adenylate uridylate-rich element · **crRNA**: CRISPR RNA · **FBS**: fetal bovine serum · **RBP**: RNA-binding protein · **RNP**: ribonuclear protein · **UTR**: untranslated region

Full correspondence: Monika C. Wolkers, Department of Hematopoiesis, Sanquin Research-AMC Landsteiner Laboratory, Plesmanlaan 125, 1066 CX Amsterdam, The Netherlands
e-mail: m.wolkers@sanquin.nl

The peer review history for this article is available at https://publons.com/publon/10.1002/eji.201948458

Received: 4/11/2019
Revised: 27/1/2020
Accepted: 27/2/2020
Accepted article online: 19/2/2020